Thin Thermoelectric Generator System for Body Energy Harvesting

KRISHNA T. SETTALURI,[1] HSINYI LO,[1,2] and RAJEEV J. RAM[1]

1.—Research Laboratory of Electronics, Massachusetts Institute of Technology, Cambridge, MA 02139, USA. 2.—e-mail: katey@mit.edu

Wearable thermoelectric generators (TEGs) harvest thermal energy generated by the body to generate useful electricity. The performance of these systems is limited by (1) the small working temperature differential between the body and ambient, (2) the desire to use natural air convection cooling on the cold side of the generator, and (3) the requirement for thin, lightweight systems that are comfortable for long-term use. Our work has focused on the design of the heat transfer system as part of the overall thermoelectric (TE) system. In particular, the small heat transfer coefficient for natural air convection results in a module thermal impedance that is smaller than that of the heat sink. In this heat-sink-limited regime, the thermal resistance of the generator should be optimized to match that of the heat sink to achieve the best performance. In addition, we have designed flat (1 mm thickness) copper heat spreaders to realize performance surpassing splayed pin heat sinks. Two-dimensional (2-D) heat spreading exploits the large surface area available in a wristband and allows patterned copper to efficiently cool the TE. A direct current (DC)/DC converter is integrated on the wristband. The system generates up to 28.5 μW/cm^2 before the converter and 8.6 μW/cm^2 after the converter, with 30% efficiency. It generates output of 4.15 V with overall thickness under 5 mm.

Key words: Thermoelectric, energy harvesting, body power, wearable, impedance matching

INTRODUCTION

Thermoelectric modules contain n-doped and p-doped semiconductor thermocouples placed electrically in series and thermally in parallel. When a temperature gradient is applied across the module, charge carriers in the doped material diffuse away from the hot side towards the cold side. This results in a potential difference across the material characterized by the Seebeck effect. The theoretical maximum power that can be generated from skin by a wearable TEG is 180 μW/cm^2,[1] assuming heat flow of 20 mW/cm^2, Z of 3×10^{-3} K^{-1}, skin temperature of 34°C, and air temperature of 22°C. Factors such as the thermal contact resistance and low natural convection coefficient in cooling the cold side yield a much smaller temperature gradient across the module.

A low-power watch powered by body heat produced 22.5 μW of electrical power with only a 1.5 K temperature drop across the TEG.[2] To further increase the heat flow in TEGs, a radiator was applied to body-powered wireless devices[3–5] and body-powered pulse oximeters.[6–8] It generated up to 100 μW of electrical power with a size of 3 cm $\times$ 3 cm $\times$ 1.5 cm.

The 2-D heat-spreading wristbands presented here produce up to 285 μW from a Bi$_2$Te$_3$ TEG module (256 thermocouples, each having 2 mm thickness and 1 mm^2 area) while maintaining total thickness <5 mm (Fig. 1a). It is thin, lightweight, and comfortable for long-term use. The infrared image in Fig. 1b shows effective cooling using the large surface area available in a wristband. Due to the high thermal conductivity of copper, heat is able to spread out and dissipate throughout the entire area, which enhances the effective heat transfer coefficient.
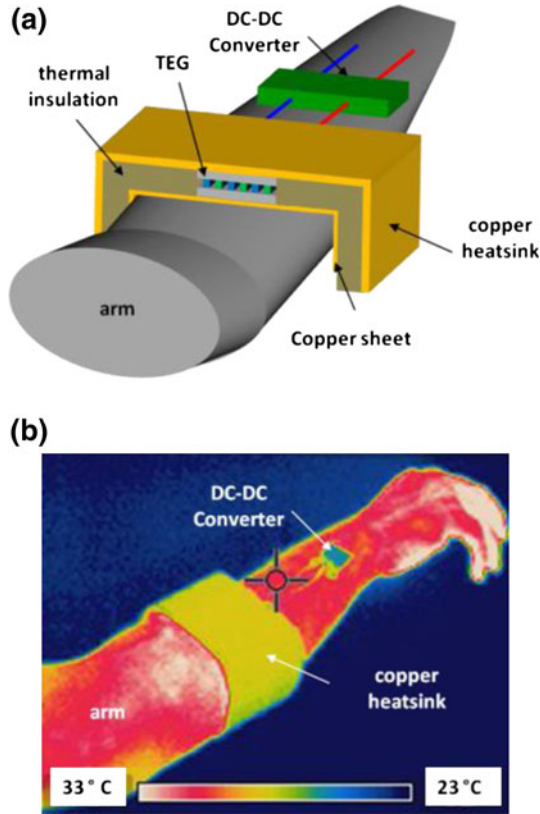
Fig. 1. (a) Schematic diagram of a low-profile wearable TEG. (b) An infrared image of copper with a high-emissivity coating showing effective cooling using the large surface area available in a wristband.

Fig. 2. Thermal resistances of heat sinks for three different convection coefficients, TIM, ceramic plates, copper sheets, and Bi_2Te_3 TE elements as a function of length.

Table I. Material properties used in the thermal resistance calculations and the simulations

	Thermal Conductivity (W/mK)	Specific Heat Capacity (J/kg K)	Density (kg/cm³)
Copper	350	385	8920
TIM	2.3	1714	2530
Ceramic	35	880	3698
Bi_2Te_3	1.6	154.4	7740

In the following, we present a design for this low-profile wearable wristband heat sink as well as an experimental prototype. The design includes thermal impedance matching and 2-D heat spreading concepts to maximize the electrical power output. We examine three types of heat sink and present experimental data compared with simulation results.

DESIGN

To estimate the temperature gradient across the TEGs, we model the system as a thermal circuit that includes a heat sink, thermal interface material (TIM), Bi_2Te_3 TE elements, ceramic plates, and copper sheet in series. The low-profile wearable heat sink is a 1-mm-thick copper plate with area of 29.2 cm × 6.4 cm. A ceramic-filled silicone TIM reduces the thermal contact resistance. A Marlow TEG module includes 256 Bi_2Te_3 thermocouples for power generation (2 mm thick, 1 mm² area) and two ceramic plates (0.7 mm thick, 10 cm² area) for electrical insulation. A flexible 0.1-mm-thick copper sheet with area of 14.6 cm × 6.4 cm is used to directly contact the skin and increase heat flow. These thermal resistances are shown in Fig. 2, as calculated using the material properties in Table I. The thermal resistances of the ceramic-filled
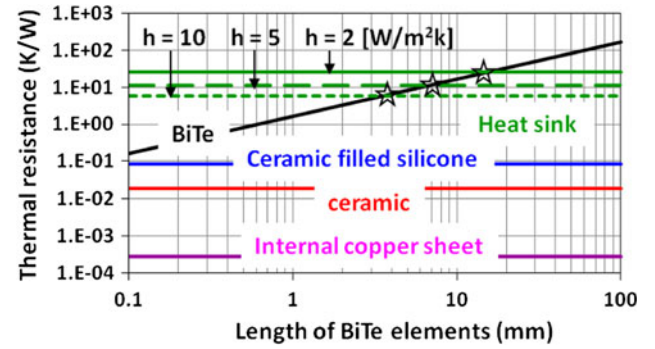
silicone, copper sheet, and ceramic plates are negligible compared with those of the heat sink and TEG. The power output (P) from the TEG can then be estimated as

$$P = \left(\frac{\Delta T \times R_{\text{th\_TEG}} \times S}{R_{\text{th\_TEG}} + R_{\text{th\_heat sink}}} \right)^2 \frac{R_{\text{el\_load}}}{\left(R_{\text{el\_heat sink}} + R_{\text{el\_load}} \right)^2},$$

where ΔT is the temperature difference between the body and ambient, S is the Seebeck coefficient, R_{el} is the electrical resistance, and R_{th} is the thermal resistance. Thermal contact resistance will be addressed later in this section.

Depending on the heat transfer coefficients, the power output can be maximized by varying the thickness of the Bi_2Te_3 elements. The model assumes thermal conductivity of 1.6 W/mK, Seebeck coefficient of 200 μV/K, and electrical conductivity of 110,000 Ω^{-1} m^{-1}. The maximum (marked with a star) is achieved when the thermal resistance of the TEGs matches that of the heat sinks, as shown in Fig. 3; that is, the temperature drop across the generator should be approximately half the total temperature drop for the entire system. This may seem counterintuitive, since one normally tries to minimize the temperature gradient across the heat sink. After choosing the best heat sink with the best heat transfer coefficient h, one needs to scale the thickness of the TEG accordingly to maximize the generated power. The optimal thickness then
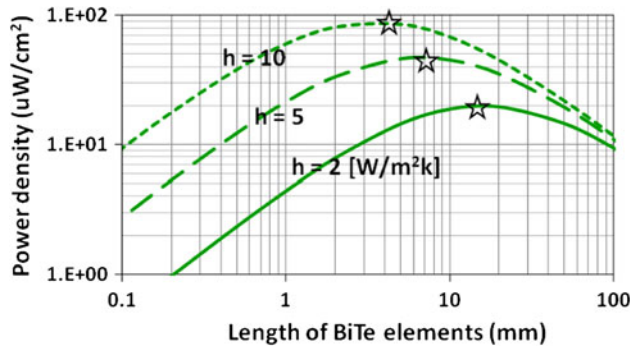
Fig. 3. Power density output assuming 10°C difference between the body and ambient as a function of the length of the Bi_2Te_3 TE elements for three convection coefficients of the heat sink.
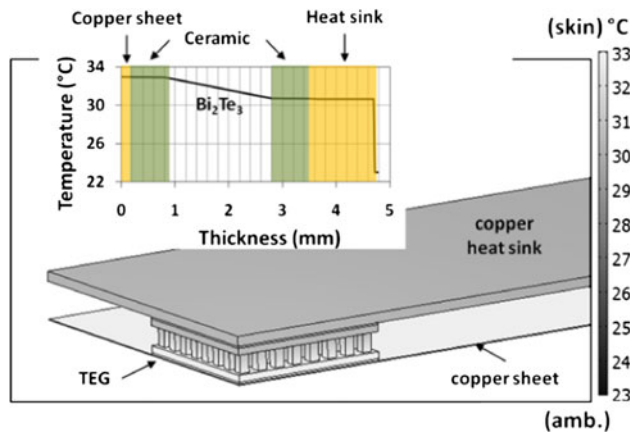

Fig. 4. Temperature distribution of the TEG system.

depends not only on the TE material parameters but also on the quality of the heat sink. A similar idea has been illustrated in Ref. 9. The number of thermocouples is chosen to match the thermal resistance of the heat sink and therefore achieve the maximum power output from the TEG. Further increases in the number of thermocouples do not increase the voltage due to the continued decrease in the TEG thermal resistance and resulting decrease in the temperature gradient across it. Optimal thermal impedance matching in the heat-sink-limited regime is also demonstrated in Refs. 10 and 11.

Aside from thermal resistance matching to maximize power output, we utilize 2-D heat spreading and create groove patterns to increase the surface area to improve the quality of the heat sink without increasing the thickness. Finite-element simulations were used to study the temperature distributions across three types of wristband heat sink, with flat, grooved, and checkerboard patterns. A constant skin temperature of 33°C was applied to the bottom of the copper sheet while the ambient temperature stayed at 23°C. Natural air convection ($h = 5$ W/m^2K) was applied on the top of the copper heat sink.
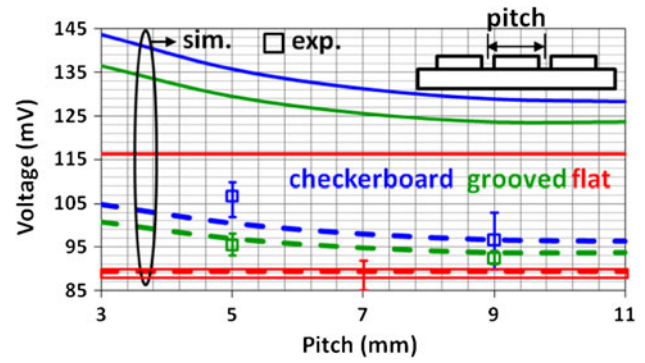

Fig. 5. Open-circuit voltage (solid: without thermal contact resistance; dashed: with thermal contact resistance of 2 K/W) as a function of groove pitch for three types of heat sink.

The TEG has the maximal temperature gradient and therefore maximal voltage immediately after contacting the skin. The body gradually heats up the TEG as well as the heat sink until the system reaches a steady state. As shown in Fig. 4, less than half of the temperature drop is within the TEG, indicating the limitation of the heat sink performance due to the low convection coefficient.

To further improve the performance of the heat sink, we created patterns on the copper plate. The output voltage as a function of groove pitch is shown in Fig. 5 (solid line). It is the product of the temperature difference across the TEG from the simulations and the Seebeck coefficient. Smaller pitches and the checkerboard pattern have larger surface areas and better heat dissipation, thereby producing higher voltage. The calculation here assumes negligible thermal contact resistance (ideal case), since precise estimation of thermal contact resistance is difficult. A reduction of the open-circuit voltage (dashed line) is expected with the present thermal contact resistance, which yields a small temperature gradient across the module. The metal–ceramic thermal contact resistance was experimentally determined to be approximately 20 cm^2 K/W. Comparison between the model with thermal contact resistance and experimental data is discussed in a later section.

FABRICATION

The prototypes in Fig. 1 were fabricated using a 1-mm copper plate with standardized dimensions of 29.2 cm × 6.4 cm. Grooves were created using a 0.5-mm-end mill bit to produce grooves with depth of 0.5 mm. Here we consider pitches of 5 mm and 9 mm. Structural instability led to a maximum groove thickness of 5 mm. Upon passing this thickness, the copper plates would frequently break when shaped using a roller. Thermal insulation (felt) was placed in the concave area of the wristband after rolling. The TEG was placed into a slot in the insulation, where the TEG has complete contact with the cold-side copper plate. It generates 50 mV for every degree of temperature across the module

itself. Lastly, an intermediate copper sheet is attached to the hot side of the TEG using the TIM, which produces greater contact between the arm and the TEG.

EXPERIMENTS AND RESULTS

Tests comparing the flat, grooved, and checkerboard wearable heat sinks were performed in an environment with constant ambient temperature and minimal air flow for natural convection. The estimated heat transfer coefficient was 5 W/m^2 K. In all tests, the heat sinks were placed on the upper forearm and the open-circuit voltage was recorded using a voltage logger (T and D VR-71) with resolution of 1 mV. Figure 6a shows plots characterizing the TEG open-circuit voltages across the hot and cold sources as a function of time for the various groove patterned heat sinks. Each heat sink was worn for 8 min under identical conditions until it reached a steady-state voltage.

For the first 10 s, the open-circuit voltage went up quickly and then started to decrease because the arm heats up the TEG and then the heat sink. Therefore, the voltage across the TEG drops until reaching a steady state. The checkerboard heat sink had the smallest heat capacity as well as the lowest thermal impedance. This results in a low thermal time constant and therefore a fast response time; that is, the voltage output for this case is more sensitive to the heat source. It goes up quickly to a maximum and then drops quickly to its steady state. The checkerboard heat sink, with the highest surface area, produced a 108 mV voltage for a 2.16 K temperature difference. The grooved and flat heat sinks produced 94 mV voltage for a 1.88 K difference and 85 mV voltage for a ~1.7 K difference, respectively.

The optimum power output from the TEG for the three types of heat sinks is plotted in Fig. 6b. Load matching occurs for a 10 Ω resistance connected to the output of the TEG; the voltage across the resistor was recorded and used to calculate the power output. The results show that the checkerboard heat sink provided 28.5 μW/cm^2 (285 μW) power output while the grooved and flat heat sinks provided 21.6 (216 μW) and 17.6 μW/cm^2 (176 μW), respectively.

A 75-min field test of the checkerboard heat sink was also performed. The TEG and checkerboard heat sink system were connected to the low-power input of a DC/DC converter (Enocean ECT100).[12] The DC/DC converter converts a source of DC energy from one voltage level to another, wasting as little as possible in the process. It contains a switch, diode, inductor, and capacitor. The entire system was worn under varying environmental conditions for 75 min. Figure 7a plots the input voltage of the DC/DC converter from the TEG and the temperature difference across the generator. The DC/DC converter open-circuit output voltage is shown in
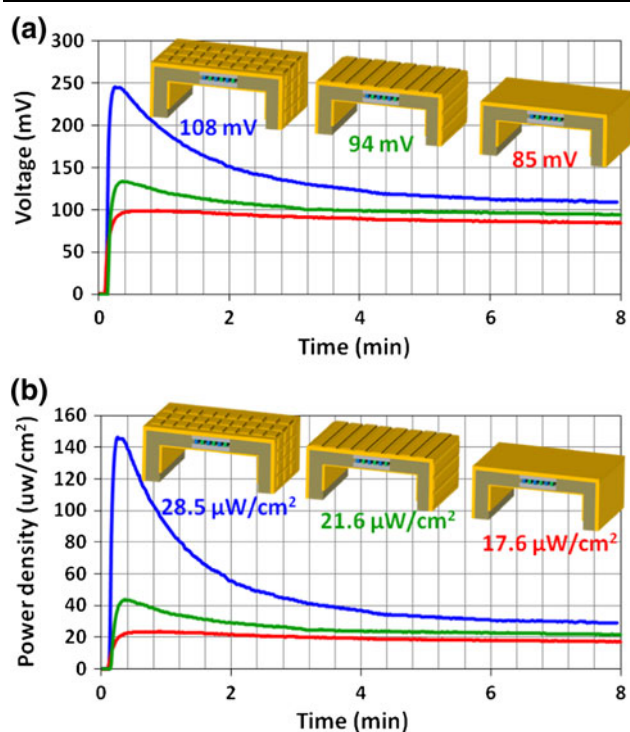

Fig. 6. (a) Measured open-circuit voltage and (b) power density as a function of time for three types of heat sink: checkerboard, grooved, and flat.
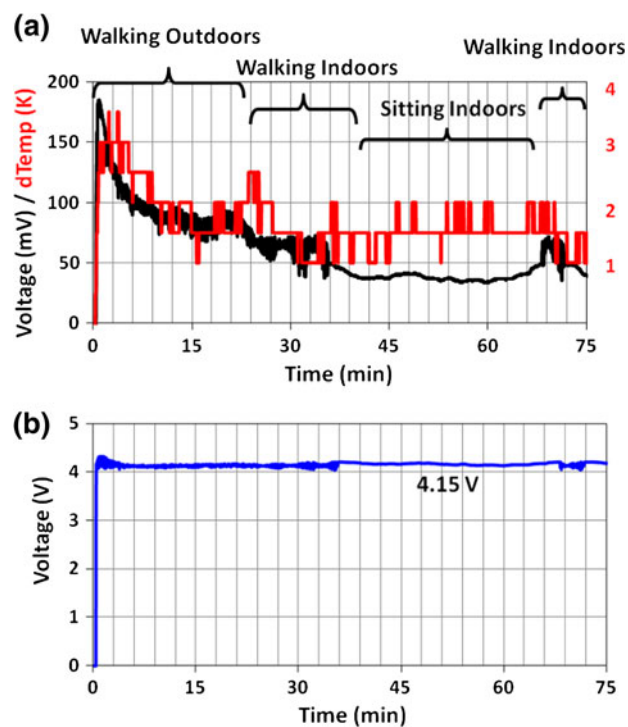

Fig. 7. (a) 75-min field test showing the voltage output and temperature difference across the TEG, which fluctuates with voltage as expected, and (b) the voltage output of the DC/DC converter during the field test.

Fig. 7b. During the 75-min test, with varying input voltages ranging from 40 mV to 180 mV, the DC/DC converter produced a consistent output voltage of 4.15 V, at 30% power efficiency.

DISCUSSION

Comparison between the experimental data and model is shown in Fig. 5. The checkerboard heat sink exhibited the best heat sink performance and generated the highest voltage and power. The denser the pitch, the higher the output voltage obtained. However, the voltage was lower than expected due to the thermal interface between copper and ceramic. The generator performance is known to depend strongly on the thermal resistance of interfaces, which is sensitive to the wristband bending to conform to the arm, deteriorating the contact between the heat sink and cold side of the module. A small air gap has been observed due to the stress created by bending. Precise estimation of thermal contact resistance is difficult, and the metal–ceramic interface was considered in the simulations (dashed lines) and validated experimentally to be about 20 cm^2 K/W. Thermal interface resistance can potentially be reduced by applying thermally conductive epoxy to secure the contact. Preliminary results with silver epoxy showed a 10% power enhancement. The checkerboard heat sink with silver epoxy provided 33.0 μW/cm^2 (330 μW) power output while that with ceramic-filled silicone provided 28.5 μW/cm^2 (285 μW) power output. However, this is an irreversible bond. Besides, realization of thermal impedance matching can be accomplished by increasing the thickness of the Bi$_2$Te$_3$ TE elements by a factor of four or reducing the thermal resistance of the heat sink by introducing forced convection.

As shown in Fig. 7a, walking increases the heat transfer coefficient by increasing convective effects. This reduces the thermal resistance of the heat sink and therefore increases the temperature gradient across the TEG. Compared with the idle condition (sitting indoors), there is less temperature variation but the voltage output is relatively lower. This further demonstrates that the quality of the heat sink is determined by the heat transfer coefficient and can be improved by human motion.

CONCLUSIONS

We introduce a low-profile wearable wristband heat sink which utilizes 2-D heat spreading rather than extending out above the hot source (skin). The heat sink is comfortable to wear and utilizes natural convection in cooling the cold side while maintaining a maximum thickness of 5 mm. The large available surface area enabled the design of flat, grooved, and checkerboard patterns on the copper plate, which showed steady-state open-circuit voltage of 85 mV, 94 mV, and 108 mV and power output of 17.6 μW/cm^2, 21.6 μW/cm^2, and 28.5 μW/cm^2, respectively.

ACKNOWLEDGEMENTS

REFERENCES

1. V. Leonov and R. Vullers, *J. Electron. Mater.* 38, 7 (2009).
2. M. Kishi, H. Nemoto, T. Hamao, M. Yamamoto, S. Sudou, M. Mandai, and S. Yamamoto, *Proceedings of International Conference on Thermoelectrics* (Baltimore, USA, 1999), pp. 301–307.
3. V. Leonov, P. Fiorini, S. Sedky, T. Torfs, and C. Van Hoof, *Proceedings of 13th International Conference on Solid-State Sensors, Actuators and Microsystems*, Vol. 1 (Seoul, Korea, 2005), pp. 291–294.
4. B. Gyselinckx, C. Van Hoof, J. Ryckaert, R. Yazicioglu, P. Fiorini, and V. Leonov, *Proceedings of the Custom Integrated Circuit Conference* (San Jose, CA, 2005), pp. 13–19.
5. V. Leonov, T. Torfs, N. Kukhar, C. Van Hoof, and R. Vullers, *Proceedings of 5th European Conference on Thermoelectrics* (Odessa, Ukraine, 2007), pp. 76–79.
6. T. Torfs, V. Leonov, C. Van Hoof, and B. Gyselinckx, *Proceedings of IEEE International Conference on Sensors* (Daegu, Korea, 2006), p. 122.
7. T. Torfs, V. Leonov, and R. Vullers, *Sensors Transducers J.* 80, 1230 (2007).
8. V. Leonov and R. Vullers, *J. Renew. Sustain. Energy* 1, 062701 (2009).
9. P. Mayer and R. Ram, *Nanoscale Microscale Thermophys. Eng.* 10, 143 (2006).
10. J. Bierschenk, *Appl. Ferroelectr.* 17, 1 (2008).
11. V. Leonov, and P. Fiorini, *Proceedings of 5th European Conference on Thermoelectrics* (Odessa, Ukraine, 2007), pp. 129–133.
12. L. Mateu, M. Pollak, and P. Spies, *Proceedings of 1st Annual nanoPower Forum* (San José, CA, 2007).